signals by pulsed microwave energy," *IEEE Trans. Microwave Theory Tech.*, vol. MTT-22, pp. 583–584, 1974.
[13] A. W. Guy, C. K. Chou, J. C. Lin, and D. Christensen, "Microwave-induced acoustic effects in mammalian auditory systems and physical materials," *Ann. NY Acad. Sci.*, vol. 247, pp. 194–218, 1975.
[14] A. H. Frey, "Human auditory system response to modulated electromagnetic energy," *J. Appl. Physiol.*, vol. 17, pp. 689–692, 1962.
[15] A. H. Frey and R. Messenger, Jr., "Human perception of illumination with pulsed ultra-high frequency electromagnetic energy," *Science*, vol. 181, pp. 356–358, 1973.
[16] C. A. Cain and W. J. Rissmann, "Microwave hearing in mammals at 3.0 GHz," selected papers from the 1975 Annual USNC/URSI Symposium, published by the Bureau of Radiological Health, in press.
[17] I. S. Sokolnikoff, *Mathematical Theory of Elasticity*, 2nd ed. New York: McGraw-Hill, 1956.
[18] A. E. H. Love, *A Treatise on the Mathematical Theory of Elasticity*. Cambridge, England: Cambridge Univ. Press, 1927.
[19] J. A. Stratton, *Electromagnetic Theory*. New York: McGraw-Hill, 1941.
[20] L. D. Landau and E. M. Lifshitz, *Electrodynamics of Continuous Media*. New York: Addison-Wesley, 1960.
[21] R. J. Knops, "A reciprocal theorem for a first order theory of electrostriction," *J. Appl. Math. and Phys. (ZAMP)*, vol. 14, pp. 148–155, 1963.
[22] H. S. Carslaw and J. C. Jaeger, *Conduction of Heat in Solids*, 2nd ed. London, England: Oxford Univ. Press, 1959.
[23] M. A. Biot, "Thermoelasticity and irreversible thermodynamics," *J. Appl. Phys.*, vol. 27, pp. 240–253, 1956.
[24] J. F. Ready, "Effects due to absorption of laser radiation," *J. Appl. Phys.*, vol. 36, pp. 462–468, 1965.
[25] A. Papoulis, *The Fourier Integral*. New York: McGraw-Hill, 1962.
[26] M. Abramowitz and I. A. Stegun, Eds., *Handbook of Mathematical Functions*, Publication no. 55, NBS-Applied Mathematics Series. Washington, DC: U.S. Government Printing Office, 1964, p. 972.

Input Impedance of Coaxial Line to Circular Waveguide Feed

M. D. DESHPANDE, STUDENT MEMBER, IEEE, AND B. N. DAS

Abstract—**The expressions for the real and imaginary parts of the input impedance seen by a coaxial line driving a thin cylindrical probe in a dominant TE_{11} mode circular waveguide are derived. The analysis is carried out by assuming that the cylindrical post is replaced by a curvilinear strip having maximum width equal to the diameter of the probe. Theoretical results on input VSWR and input impedance seen by a coaxial line are in close agreement with experimental data.**

I. Introduction

ELECTROMAGNETIC ENERGY is coupled to a waveguide by means of a probe or loop radiators driven from a source through a coaxial line. A rigorous solution of the problem of a cylindrical probe parallel to the electric field in a rectangular waveguide has been presented by Collin [1]. Harrington [2] has found a method for determining an equivalent network of the junction between a coaxial line and a rectangular waveguide and has determined the resistive part of the input impedance seen by a coaxial line from the stationary formula for the impedance. An analysis for the determination of variation of both resistive and reactive parts of the input impedance for a cylindrical probe exciting a circular cylindrical waveguide has not been reported in the literature.

In this paper, expressions for the real and imaginary parts of the input impedance seen by a coaxial line driving a cylindrical probe in a dominant TE_{11} mode circular waveguide are derived. Assumption of a purely filamentary radial probe leads to a divergent series for the imaginary part of the input impedance [2]. For the purpose of analysis the thin cylindrical probe is assumed to be replaced by a curvilinear metallic strip in the cross section of the waveguide. This assumption simplifies the analysis considerably and leads to an expression for the imaginary part of the input impedance in the form of an infinite series which is convergent. A formula for the input impedance seen by a coaxial line is derived for a circular cylindrical waveguide terminated in a matched load on one side and in a short circuit at a distance L_1 from the probe on the other side. The expressions for the parameters of the equivalent network of the junction are also derived.

The variation of the input impedance with frequency seen by a coaxial line is computed for probe length l, $0.6 \leq l \leq 0.8$ cm, probe diameter $d = 0.2$ cm, and $0.7 \leq L_1 \leq 1.0$ cm. The theoretical results on variation of the input impedance seen by a coaxial line and the VSWR in a coaxial line are in close agreement with the experimental data for a radial probe having a diameter equal to the maximum width of the curvilinear strip.

Manuscript received September 14, 1976; revised April 20, 1977.
The authors are with the Department of Electronics and Electrical Communication Engineering, Indian Institute of Technology, Kharagpur 721302, India.

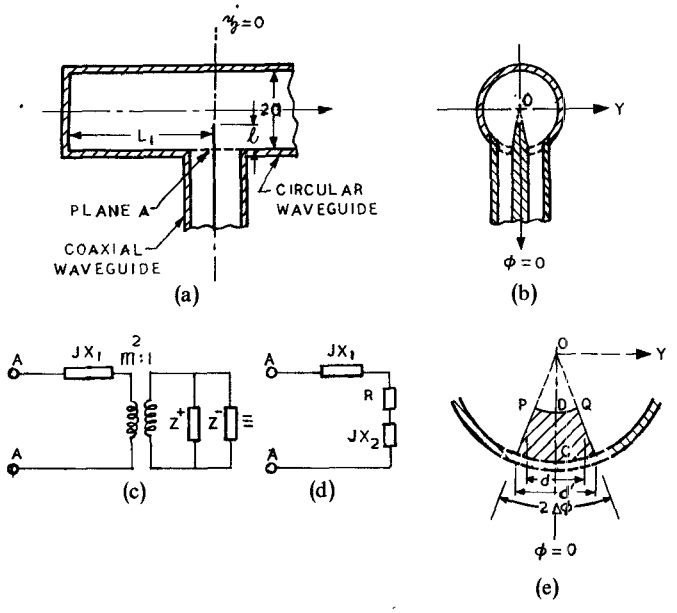

Fig. 1. Coaxial line to circular waveguide feed. (a) Longitudinal section. (b) Transverse section. (c) and (d) Equivalent circuit. (e) Exploded view of Fig. 1(b).

II. Analysis

Fig. 1(a) shows a coaxial line which drives a thin cylindrical probe in a dominant TE_{11} mode circular waveguide. For convenience in the analysis the probe in the circular waveguide is assumed to be replaced by a curvilinear strip in the cross section ($z = 0$ plane) of the waveguide as shown in Fig. 1(b). An equivalent circuit useful for calculation of the input impedance seen by a coaxial line when one mode propagates is shown in Fig. 1(c), in which input impedance Z^+ for $z = 0$ appears in parallel with input impedance $Z^- = JX'$ for $z = 0$. An expanded view of the strip of Fig. 1(b) is shown in Fig. 1(e).

The parameters of the equivalent circuit (Fig. 1(c)) can be determined from the stationary formula for the input impedance seen by a coaxial line [2], which is given by

$$Z_{in}|_A = \frac{1}{I_{in}^2} \sum_{i=0} \frac{Z_i \left(\iint_{\text{cross section}} J_s \cdot e_i \, ds \right)^2}{(1-\Gamma_i^-)(1+\Gamma_i^-)^{-1} + (1-\Gamma_i^+)(1+\Gamma_i^+)^{-1}} \tag{1}$$

where J_s is the surface current in the cross-section plane $z = 0$, Z_i is the modal impedance, e_i is the normalized vector mode function, Γ_i^+ and Γ_i^- are, respectively, the $+z$ and $-z$ reflection coefficients for the ith mode, and I_{in} is the input current at reference plane A. Since the waveguide supports only the dominant mode ($i = 0$), Z_i is real for $i = 0$ and imaginary for $i \neq 0$. Further, $\Gamma_i = 0$ for $i \neq 0$. Equation (1) can now be simplified to the form

$$Z_{in}|_A = m^2 \frac{Z^+ Z^-}{Z^+ + Z^-} + jX_1 \tag{2a}$$

where

$$m^2 = \frac{1}{I_{in}^2} \left(\iint_{\text{cross section}} J_s \cdot e_0 \, ds \right)^2 \tag{2b}$$

$$X_1 = \frac{1}{2I_{in}^2} \sum_{i \neq 0}^{\infty} Z_i \left(\iint_{\text{cross section}} J_s \cdot e_i \, ds \right)^2 \tag{2c}$$

$$Z^+ = Z_0$$

and

$$Z^- = jZ_0 \tan(\beta_0 L_1)$$

β_0 being the propagation constant for the $i = 0$ mode.

In order to determine $Z_{in}|_A$ and the equivalent circuit of the junction, it is necessary to determine J_s for $z = 0$.

III. Expression for Current Distribution

In the coordinate system shown in Fig. 1 the probe length extends from point D ($\rho = a - l$) to point C ($\rho = a$). The distribution of the trial current in the curvilinear strip of Fig. 1(e) is assumed to be uniform in the ϕ direction and to have a sinusoidal distribution of the form

$$I(\zeta) = I_0 \sin K(l - \zeta)$$

in the radial direction. In the above expression $K = 2\pi/\lambda$ and ζ is the variable along the line CDO. For the configuration shown in Fig. 1(e), the variable ζ for points D and C is 0 and l, respectively. In the linear segment CD a relation of the form $\zeta = A\rho + B$ may be assumed. Evaluating the constants A and B from the values of ξ and ρ at points D and C, the relation between ζ and ρ is obtained as $\xi = -\rho + a$. The current distribution, therefore, takes the form

$$I(\rho) = I_0 \sin K(l - a + \rho).$$

For the purpose of calculating J_s, it will be assumed that the diameter d of the probe is equal to the average between the maximum and minimum widths of the curvilinear strip. For a thin cylindrical probe of length l and diameter d in a circular cylindrical waveguide of diameter $2a$ the surface current in the cross section $z = 0$ can, therefore, be assumed to be of the form

$$J_s = u_\rho \frac{I_0}{d} \sin K(l - a + \rho), \qquad \text{for } -\Delta\phi \leq \phi \leq \Delta\phi$$

$$J_s = 0, \qquad \text{elsewhere} \tag{3a}$$

where

$$\Delta\phi = d'/2a \approx d/2a. \tag{3b}$$

Since the expression for the input impedance is stationary in character [2] the error produced due to this assumption is small.

IV. Expression for the Real and Imaginary Parts of the Input Impedance

The parameters m^2 and X_1 of the equivalent circuit shown in Fig. 1(c) are determined by using (3a) and the ortho-

normalized vector mode functions for the mode of index n_1p ($i \equiv n,p$) derived by Harrington [2]. The vector mode function e^e_{11} for the dominant TE_{11} mode of a circular waveguide is given by

$$e^e_{11} = \sqrt{\frac{2}{\pi(x'^2_{11}-1)}}\frac{1}{J_1(x'_{11})} \cdot \left[-u_\rho \frac{1}{\rho} J_1(x'_{11}(\rho/a)) \cos\phi + u_\phi \frac{x'_{11}}{a} J'_1(x'_{11}(\rho/a)) \sin\phi\right]. \quad (4a)$$

The vector mode functions e^e_{np} for TE modes and e^m_{np} for TM modes are given by

$$e^e_{np} = \sqrt{\frac{2\varepsilon_n}{\pi(x'^2_{np}-n^2)}}\frac{1}{J_n(x'_{np})} \cdot \left[-u_\rho \frac{n}{\rho} J_n(x'_{np}(\rho/a)) \sin(n\phi) + u_\phi \frac{x'_{np}}{a} J'_n(x'_{np}(\rho/a)) \cos(n\phi)\right] \quad (4b)$$

$$e^m_{np} = -\sqrt{\frac{\varepsilon_n}{\pi}}\frac{1}{x_{np}J_{n+1}(x_{np})} \cdot \left[u_\rho \frac{x_{np}}{a} J'_n(x_{np}(\rho/a)) \cos(n\phi) - u_\phi \frac{n}{\rho} J_n(x_{np}(\rho/a)) \sin(n\phi)\right] \quad (4c)$$

where $\varepsilon_n = 1$ for $n = 0$, $\varepsilon_n = 2$ for $n = 2$. x'_{np} is the pth root of $dJ_n(x)/dx = 0$ and x_{np} is the pth root of $J_n(x) = 0$.

Substituting (4a,b,c) into (2b) and (2c) the surface integrals appearing in the expression for equivalent circuit parameters m^2 and X_1 split into the product of two integrals; integration with respect to variable ϕ and integration with respect to variable ρ. The integration with respect to variable ϕ appears in the form

$$\int_{-\Delta\phi}^{\Delta\phi} \cos\phi\, d\phi \qquad \int_{-\Delta\phi}^{\Delta\phi} \cos(n\phi)\, d\phi \qquad \int_{-\Delta\phi}^{\Delta\phi} \sin(n\phi)\, d\phi$$

which is expressed in the closed form. The integration with respect to variable ρ, however, cannot be evaluated in the closed form. The expressions for m^2 and X_1 are, therefore, found to be

$$m^2 = \frac{2}{\pi(x'^2_{11}-1)}\frac{1}{\sin^2(Kl)J^2_1(x'_{11})}\left[\frac{\sin(d'/2a)}{(d'/2a)}\right]^2 \cdot \left[\int_{1-l/a}^{1} \sin[Ka(l/a-1+x)]J_1(x'_{11}x)\, dx\right]^2 \quad (5)$$

$$X_1 = -\sum_{n=0}\sum_{p=1}\frac{\sigma_0\varepsilon_n}{J^2_{n+1}(x_{np})}\frac{\sqrt{(x_{np}/Ka)^2-1}}{\sin^2(Kl)}\left[\frac{\sin(nd'/2a)}{(nd'/2a)}\right]^2 \cdot \left[\int_{1-l/a}^{1} \sin[Ka(l/a-1+x)J_n(x_{np}x)x\, dx\right]^2. \quad (6)$$

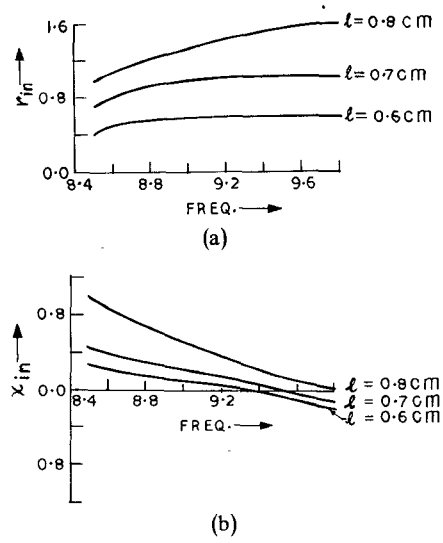

Fig. 2. Variation of the normalized input impedance versus frequency with l as a parameter for $L_1 = 1.0$ cm. (a) Real part of the input impedance. (b) Imaginary part of the input impedance.

For the calculation of the input impedance seen by the coaxial line, the equivalent circuit of Fig. 1(c) is reduced to the form shown in Fig. 1(d). The expressions for the real and imaginary parts of the input impedance normalized with respect to the characteristic impedance, $Z_{oc} = 50\ \Omega$, of the coaxial line are given by

$$\gamma_{in} = R_{in}/Z_{oc} = \frac{m^2 Z_0 \tan^2(\beta_0 L_1)}{Z_{oc}(1+\tan^2(\beta_0 L_1))} \quad (7a)$$

$$jx_{in} = jX_{in}/Z_{oc} = j(X_2 + X_1)/Z_{oc} \quad (7b)$$

where

$$jX_2 = j\frac{m^2 Z_0 \tan(\beta_0 L_1)}{[1+\tan^2(\beta_0 L_1)]}. \quad (7c)$$

The line integrals appearing in the expression for m^2 and jX_1 are numerically evaluated. The magnitude of reflection coefficient at reference plane A seen by the coaxial line is

$$|\Gamma| = \frac{\sqrt{\gamma^2_{in}+x^2_{in}}-1}{\sqrt{\gamma^2_{in}+x^2_{in}}+1} \quad (8)$$

and, the VSWR in the coaxial line is given by

$$\text{VSWR} = \frac{1+|\Gamma|}{1-|\Gamma|}. \quad (9)$$

The various quantities related to the design of transition are evaluated by using (7)–(9).

It is found from the expressions (7a) and (7b) that the input impedance seen by the coaxial line is a function of the length of the probe, the distance L_1 of the conducting plate from the probe, and the frequency of operation. For $a = 1.15$ cm, $d = d' = 0.2$ cm, $L_1 = 1.0$ cm, and $l = 0.6, 0.7$, and 0.8 cm, the variations of r_{in} and x_{in} with frequency evaluated from (7a,b,c) and (8) are presented in Fig. 2. For $l = 0.7$ cm and $L_1 = 0.7$, 0.8, 0.9, and 1.0 cm, the computed results on the variations of r_{in} and x_{in} with frequency are shown in Fig. 3. It is evident from Figs. 2 and 3 that for $l = 0.7$ cm and $L_1 \approx 1.0$

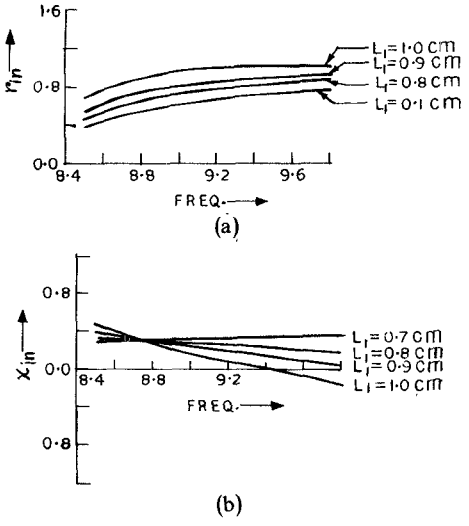

Fig. 3. Variation of the normalized input impedance versus frequency with L_1 as a parameter for $l = 0.7$ cm. (a) Real part of the input impedance. (b) Imaginary part of the input impedance.

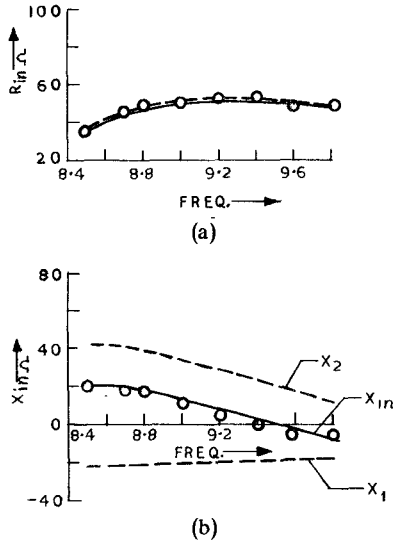

Fig. 4. Variation of input impedance versus frequency for $l = 0.7$ cm and $L_1 = 1.0$ cm. (a) Real part of the input impedance. (b) Imaginary part of the input impedance. Theory ———. Experiment 0——0.

cm the VSWR in the coaxial line has a low value over a relatively large frequency range.

A transition with $a = 1.15$ cm, $d = 0.2$ cm, $l = 0.7$ cm, and $L_1 \approx 1.0$ cm is fabricated. Using (6) and (7a,b,c), the variation of the parameters of the equivalent circuit of Fig. 1(d) with frequency are evaluated and presented in Fig. 4. The reactance jX_1 in the equivalent circuit results from the energy stored in the evanescent modes generated by the probe current, and is capacitive in nature. The reactance jX_2 depends upon the position of the short-circuiting plunger. For $L_1 \approx 1.0$ cm and a frequency range of 8.5–9.8 GHz, jX_2 is inductive. A comparison between the theoretical and experimental results on the total input impedance in ohms seen by the coaxial line is also presented in the Fig. 4. The experimental results on the variation of the input VSWR with frequency is plotted in Fig. 5 together with the computed results obtained from (7a,b,c)–(9).

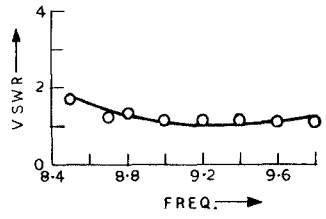

Fig. 5. Variation of the input VSWR versus frequency for $l = 0.7$ cm and $L_1 = 1.0$ cm. Theory ———. Experiment 0——0.

V. Conclusion

In spite of the approximation made in the analysis, there is a close agreement between the theoretical and experimental results. In the frequency range 9.0–9.8 GHz the minimum VSWR is less than 1.2. The frequency at which the reactive part of the input impedance is zero is a function of the length of probe and the position of the shorting plunger.

For a filamentary current exciting the waveguide, the summation for jX_1 diverges. Assumption of a curvilinear strip leads to a rapidly convergent series for jX_1. It is found that the evanescent modes with $p = 1$ and $n = 0, 1, 2, 3, \cdots$, 12 make a significant contribution to the reactive part of the input impedance. The contribution of the evanescent modes with higher values of p is found to be quite small. If the short circuit at $z = -L_1$ is replaced by a matched load the reactive part of the input impedance is jX_1 which is capacitive in nature. In the presence of a short circuit the reactance jX' appearing in Fig. 1(c) is inductive for values of $0° \leq \beta_0 L_1 \leq 90°$. For $0° \leq \beta_0 L_1 \leq 45°$ the reactance curve for jX_2 has a positive slope while for $45° \leq \beta_0 L_1 \leq 90°$ it has a negative slope and for $\beta_0 L_1 = 45°$ it has zero slope. For $L_1 = 1.0$ cm and a frequency range of 8.5–9.8 GHz, $\beta_0 L_1$ lies between 45 and 74°. Since over this frequency range variation in jX_1 is very small and the curve for jX_2 has a negative slope, the input reactance shows a negative slope with frequency.

Acknowledgment

The authors would like to thank Prof. G. S. Sanyal and Prof. J. Das for their kind interest in the work.

References

[1] R. E. Collin, *Field Theory of Guided Waves*. New York: McGraw-Hill, 1960, ch. 7, pp. 258–307.
[2] R. F. Harrington, *Time Harmonic Electromagnetic Field*. New York: McGraw-Hill, 1961, ch. 8, pp. 381–440.